Irradiation effects of CO_2 laser parameters on surface morphology of fused silica*

Xiang Xia(向 霞)[a)b)], Zheng Wan-Guo(郑万国)[a)], Yuan Xiao-Dong(袁晓东)[a)†], Dai Wei(戴 威)[a)b)], Jiang Yong(蒋 勇)[a)b)], Li Xi-Bin(李熙斌)[a)], Wang Hai-Jun(王海军)[a)], Lü Hai-Bing(吕海兵)[a)], and Zu Xiao-Tao(祖小涛)[b)]

[a)] *Research Centre of Laser Fusion, China Academy of Engineering Physics, Mianyang* 621900, *China*

[b)] *Department of Applied Physics, University of Electronic Science and Technology of China, Chengdu* 610054, *China*

(Received 9 August 2010; revised manuscript received 12 September 2010)

To understand the surface morphology evolution of fused silica induced by 10.6-μm CO_2 laser irradiation at different parameters, this paper reports that optical microscopy, profilometry, and hydrophilicity tests are utilized to characterize the surface structure and roughness of the laser irradiated area. The results show that three typical surface morphologies and two typical hydrophilicity test images are observed at different laser powers and pulse durations. The correlations between surface temperature and surface morphology as well as hydrophilicity behaviours are presented. The different hydrophilicity behaviours are related to surface structures of the laser-induced crater and thermal diffusion area. The thermal diffusion length monotonously increases with increasing laser power and pulse duration. The crater width is almost determined by the laser beam size. The crater depth is more sensitive to the laser power and pulse duration than the crater width.

Keywords: CO_2 laser irradiation, fused silica, surface structure, hydrophilicity

PACS: 42.70.Ce, 78.20.–e, 78.55.Qr, 79.20.Eb **DOI:** 10.1088/1674-1056/20/4/044208

1. Introduction

Fused silica is a preferred optical material for high-fluence optics in many laser applications because its high bulk purity leads to low absorption in a wide spectral range, resistance to laser damage, and good thermal and mechanical stability. Although the dielectric breakdown threshold of pure bulk fused silica is very high, the laser-induced damage threshold (LIDT) of the surface is much lower. Due to the surface and subsurface defects induced by grinding and polishing, the interaction of high-power laser radiation with optical-material surfaces is distinctly different from interaction with the material's bulk in light absorption, intensity pattern formation, and absorbed energy dissipation.[1−4] The surface damage resistance of fused silica optics has been the subject of extensive studies in high-power laser facilities, such as the National Ignition Facility (NIF) in the USA and the megajoule laser in France. Although the surface damage initiated at 3ω on NIF silica optics will encompass only a fractional area, studies have shown that the damage can grow rapidly with the number of shots at a laser fluence of 5 J/cm^2 to 6 J/cm^2, which is just a factor of two below the LIDT of a pristine silica surface.[5,6] Therefore, mitigation of surface damage growth is essential for the lifetime extension of the expensive large-scale laser optics when the surface damage is small.

Four methods for mitigating surface damage growth on fused silica optics have been studied, including wet chemical etching, cold plasma etching, CO_2 laser processing, and microflame torch processing. Among them, CO_2 laser processing is the best mitigation method, which gives the most consistent and convincing results.[7,8] Much attention is thus paid to studies on surface damage mitigation of fused silica by a CO_2 laser. The theoretical studies focus on the simulations of temperature and stress distributions generated by CO_2 laser processing.[9−11] In most experimental investigations, the mitigation technique has been improved for engineering purposes. For instance, Bass *et al.* reported the mitigation of damage sites larger than 100 μm with a galvanometer scanned CO_2 laser and a vacuum nozzle assembly designed to reduce the amount of evaporated fused sil-

*Project supported by the National High Technology Research and Development Program of China (Grant No. 2008AA8040508) and the Foundation for Young Scholars of University of Electronic Science and Technology of China (Grant No. L08010401JX0806).

†Corresponding author. E-mail: yxd66my@163.com

© 2011 Chinese Physical Society and IOP Publishing Ltd

ica that re-deposits or re-condenses as debris on the surface during the mitigation process.[12,13] During *et al.* presented a new set-up to study the mitigation of laser damage by varying the spatial profile of the CO_2 laser beam to increase the efficiency of the mitigation technique.[14] Guss *et al.* also investigated the damage mitigation by using a CO_2 laser operating at 4.6-μm wavelength. The damage sites as large as 500 μm in diameter with cracks extending to 200 μm in depth were successfully mitigated.[15] In this work, the evolution of surface morphology has been investigated at different CO_2 laser parameters by optical microscopy, profilometry, and hydrophilicity tests. Three types of surface morphologies and two types of hydrophilicity test images are observed at different laser powers and pulse durations. The thermal diffusion length, the crater width and the depth are also studied.

2. Experimental

Optically polished fused silica flat substrates, 40 nm ×40 nm ×5 mm, are used in this work. The material is Corning 7980 synthetic amorphous silicon dioxide, with low concentration oxygen vacancies and good transparency in the UV-visible waveband. The polished samples have root-mean-square roughness of 0.53 nm and 16 nm. Before laser irradiation, the samples are ultrasonically cleaned with deionized water and chemically etched with a buffered hydrofluoric acid (1% HF, 15% NH_4F) solution in order to remove surface contamination and re-deposited polishing materials.

A continuous wave carbon dioxide laser (Coherent GEM-100L) with a 100-W maximum power is used for the laser irradiation of fused silica substrates. The emission wavelength is 10.6 μm, which is mostly absorbed by silica with an absorption fraction of 85%.[9] The spatial mode of emission is a TEM_{00} near-Gaussian beam and it is focused on the fused silica sample with a commercial Zinc Selenide lens. The beam at the sample plane is an elliptical spot, with a long axis 700 μm and short axis 500 μm at $1/e^2$ as measured by the knife edge method. The laser frequency, power, and pulse duration are externally adjusted by a computer. In this experiment, the frequency is kept at 100 Hz and the power control is achieved by changing the duty cycle. The correlation between the duty cycle and the laser power is measured by a coherent power meter and plotted in Fig. 1. The laser power increases linearly with the duty cycle. In this work, the laser power is controlled below 30 W (corresponding to a duty cycle of 20%) and the pulse duration ranges from 100 ms to 250 ms. After laser irradiation, a circular crater is created on the fused silica surface. To understand the laser parameter dependence of the crater size, a Nikon optical microscope and a Zygo profilometer are utilized to characterize the surface morphology and roughness. The surface structure evolution induced by laser irradiation is characterized by the hydrophilicity. The irradiated samples are mounted on a beaker with boiling water inside and then observed by an optical microscope immediately to obtain the water–vapour adsorption images.

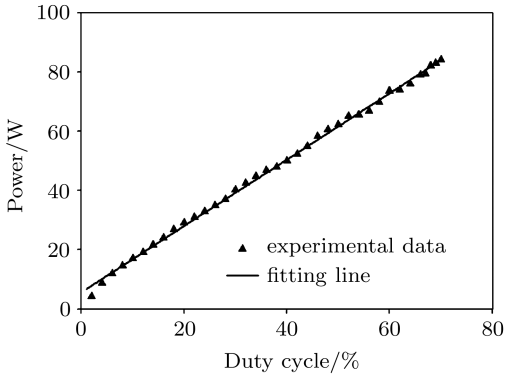


Fig. 1. Measured laser power as a function of duty cycle of the CO_2 laser used for experiments.

3. Results and discussion

Various CO_2 laser powers and pulse durations result in different surface morphologies. In this work, three typical surface morphologies are observed in the laser irradiated areas of fused silica, as shown in Fig. 2. When the laser power is small, there is no visible distortion on the surface, even after long irradiation time, e.g., 4% duty cycle and 200-ms pulse duration (Fig. 2(a)). Although 85% CO_2 laser energy can be absorbed by fused silica,[9] the thermal convection between the sample surface and ambient air keeps the temperature below, or at, the softening point of silica ($T \leq T_s$). In this way, laser irradiation hardly induces obvious surface distortion except heating of the sample. With an increase in laser power, the surface distortion occurs due to softening silica substrate induced by CO_2 laser irradiation (Fig. 2(b), 7% and 170 ms). In other words, the surface temperature is above the softening point of fused silica and below the evaporation point ($T_s < T < T_e$). When the pulse duration is longer, the surface distortion becomes clearer and a black ring appears around it (Fig. 2(c), 7% and 200 ms). Similar distortion surrounded by a black

ring can also be observed when the laser power increases. The black ring has been identified as the debris re-deposited or re-condensed from evaporated fused silica.[12] The debris is composed of the SiO_x ($0 < x < 2$) species with a nonstoichiometric formula, which could induce a decrease in LIDT by absorbing photons in the visible region and local enhancement of roughness.[6] The optical properties of the nonstoichiometric SiO_x species have also been studied in previous work.[16,17] Anyway, the black ring indicates that the surface temperature is above the evaporation point of fused silica ($T > T_e$).

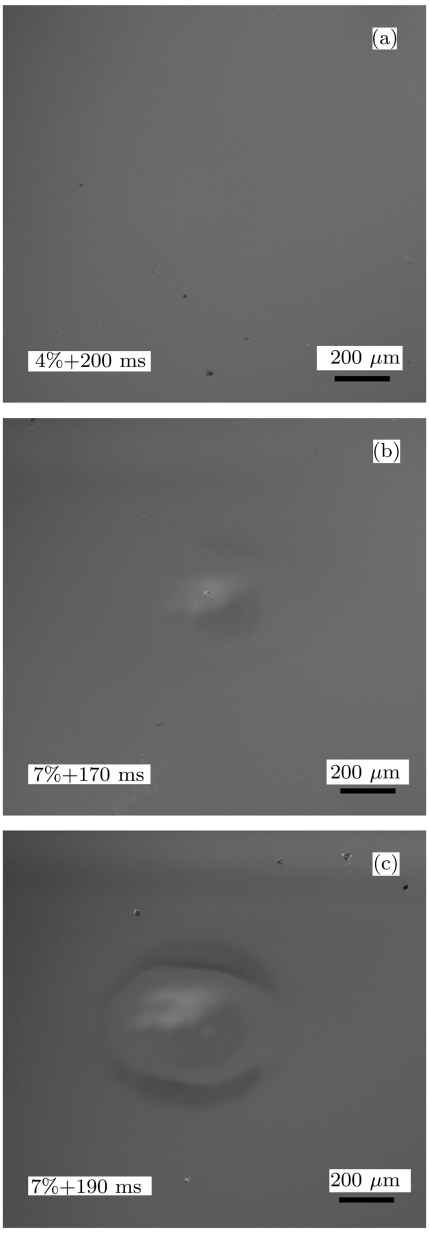


Fig. 2. Three typical surface morphologies observed in the laser irradiated areas of fused silica: (a) $T \leq T_s$, (b) $T_s < T < T_e$, (c) $T > T_e$.

The hydrophilicity test results indicate two kinds of typical water-vapour adsorption images shown in Fig. 3. The images correspond to Figs. 2(a) and 2(c). The water-vapour adsorption image of Fig. 2(b) is similar to that of Fig. 2(c). The un-irradiated area is uniformly covered by a large number of very small water droplets. More water vapour condenses around the defects, which can be observed in Figs. 2(a) and 2(c). In Fig. 3(a), an elliptical area covered with larger water droplets appeared in the laser irradiated zone. The long axis is about 800 μm and the short axis 600 μm. In Fig. 3(b), a water droplet ring (1450 μm × 1200 μm) is also observed around the elliptical area (630 μm × 420 μm). In addition, a water film forms between the elliptical area and the droplet ring. The results show that the surface structure evolution occurs when different laser power and irradiation times are used. According to all hydrophilicity test images in this work, it could be deduced that there is only one elliptical area covered with larger water droplets when the surface temperature is below, or at, the softening point of silica ($T \leq T_s$). When the temperature is above T_s, an elliptical area and a water droplet ring are observed.

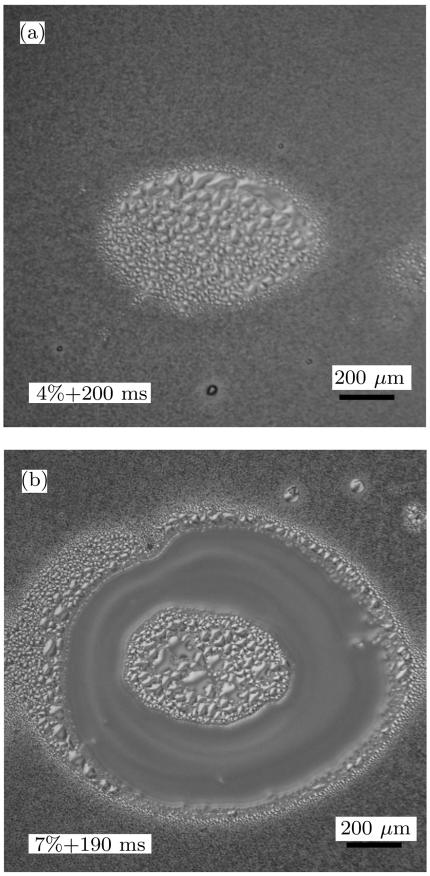


Fig. 3. Two typical water-vapour adsorption images by a hydrophilicity test of the laser irradiated areas: (a) $T \leq T_s$, (b) $T > T_s$.

In order to understand the correlation between different hydrophilic behaviours and surface morphologies, the corresponding depth profiles of the laser irradiated areas measured by the profilometer are given in Fig. 4. After laser irradiation, a crater formed in the substrate surface, whose depth depends on the laser parameters. The crater depth will be discussed later. Here, attention is focused on the crater width. For the crater created by the laser at 4% duty cycle and 200-ms pulse duration, the depth is about 25 nm and the horizontal width is 500 μm (Fig. 4(a)). At a 7% duty cycle and 200-ms pulse duration, the crater depth and horizontal width increase to ∼130 nm and 650 μm, respectively (Fig. 4(b)). It seems that the crater width is related to the long axis of the elliptical area in Fig. 3(b). Actually, by comparison of hydrophilicity test images and depth profiles of all laser irradiated areas, it is found that the horizontal width of the elliptical area is almost the same as the width of the crater when the surface temperature is larger than T_s. In addition, the crater width nearly keeps constant at different laser powers and irradiation times, as shown in Fig. 5. Therefore, the elliptical area in Fig. 3(b) corresponds to the directly irradiated area by the elliptical laser spot (700 μm × 500 μm), i.e., the crater width is determined by the laser beam size and shape. In the crater area, the surface roughness induced by distorted morphology is large, where the larger water droplets tend to accumulate to form an elliptical area. As for the droplet ring whose size is larger than the laser spot size, it should be the boundary of the thermal diffusion area. It is known that a CO_2 laser can be strongly absorbed by silica, so it is often used for surface polishing[18,19] besides softening or vaporizing the offending materials in a fused silica surface. The thermal diffusion area is actually polished by the diffused CO_2 laser energy. Therefore, the area becomes smoother than the pristine substrate surface. As a result, a layer of uniform water film appears between the crater area and the droplet ring (Fig. 3(b)). After comparing Fig. 3(a) with Fig. 4(a), one can find that the width of the droplet-covered elliptical area (800 μm) is larger than the laser spot (700 μm) and crater width (500 μm). This is because both the crater depth and the thermal diffusion length are small at low laser power and short irradiation time. In other words, when the surface temperature $T \leq T_s$, the laser irradiated area and thermal diffusion area mix together, so only one droplet-covered area is observed.

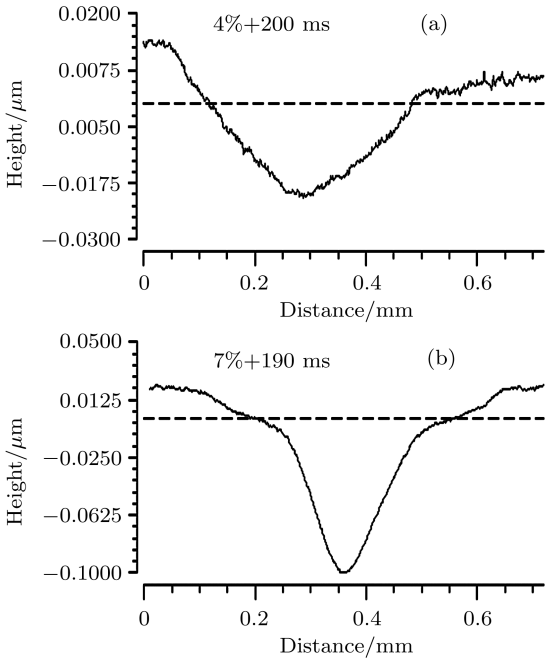


Fig. 4. Depth profiles of laser irradiated areas corresponding to Fig. 3.

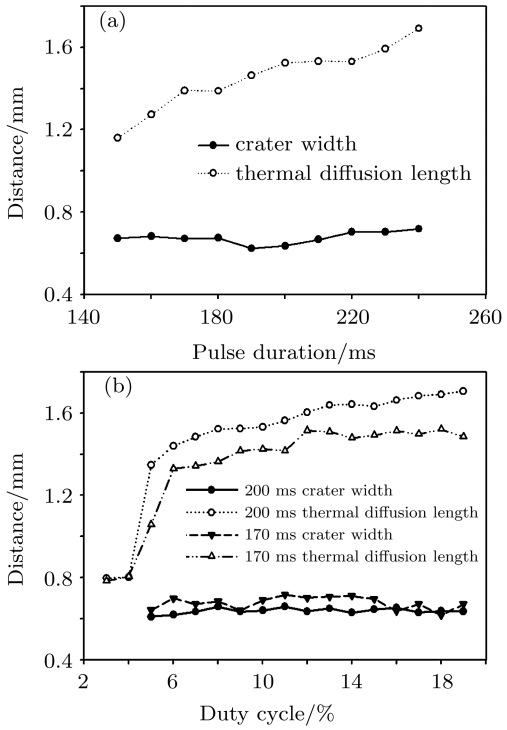


Fig. 5. Crater width and thermal diffusion length as a function of (a) pulse duration (duty cycle = 7%) and (b) duty cycle (pulse duration = 170 ms and 200 ms).

The crater width and thermal diffusion length are analysed at different duty cycles (laser powers) and irradiation times by the hydrophilicity test images. Figure 5(a) shows the relationships between pulse duration and crater width as well as thermal diffusion length when the duty cycle is 7%. At this duty cy-

cle, the crater and diffusion areas can be separated when the pulse duration $\geq$ 150 ms. The crater width is almost constant when the laser parameters used are those shown in Fig. 5(a). The fluctuation may be due to the measurement error or laser power stability. This is consistent with Palmier's study,[20] in which the crater diameter is independent of the pulse length. The thermal diffusion length monotonously increases with the pulse duration when the laser power does not change. Figure 5(b) shows the correlations between duty cycle and crater width as well as thermal diffusion length when the pulse duration is 170 ms and 200 ms, respectively. The crater width also keeps constant and the diffusion length increases with the increasing duty cycle. When the duty cycle is less than 5%, the crater width cannot be separated from the thermal diffusion length, so there is no crater data for 3% and 4%. Palmier *et al.* reported that the crater diameter increases linearly with the laser power, and the CO_2 laser beam diameter also increased when the power increased in their work.[20] However, in this work, the laser beam size remains stable at 700 μm × 500 μm, and there is no obvious increase in crater width observed when the laser power increases. Therefore, the crater width is mostly determined by the laser beam size.

Besides the transverse dimension, the crater depth profile is also studied at different duty cycles and irradiation times by the profilometer. In the laser irradiated area, the peak-valley (PV) roughness could be regarded as the crater depth. Figure 6 shows the PV roughness data at different duty cycles and pulse durations. The results show that both duty cycle and pulse duration have a significant influence on the crater depth. This is not the same as the crater width, which almost keeps constant at different parameters (Fig. 5). But the trend is consistent with previous experimental and calculated results.[20] Actually, both the crater width and depth are up to the laser energy deposition as well as temperature distribution on the transverse and longitudinal directions of the silica substrate, respectively. In the transverse direction, because of the silica's poor thermal conductivity (1.38 W/(m·K) at 20 °C and 2.68 W/(m·K) at 900 °C), most deposited energy and high temperature are probably restricted within the laser spot area. However, in the longitudinal direction, besides thermal conductance, the refractive index and absorption coefficient also contribute much to the energy deposition and temperature distribution. McLachlan and his co-workers reported that the absorption depth of the CO_2 laser radiation varies significantly with temperature, from 34 μm at 25 °C to 4 μm at 1800 °C.[21] According to the calculations by Feit *et al.*, high temperatures (3500 °C) could extend 40 μm into silica at a laser energy of 28 J/cm^2 and pulse length of 50 μs.[9,10] This may be why the crater depth is more sensitive to the laser power and pulse duration than the crater width.

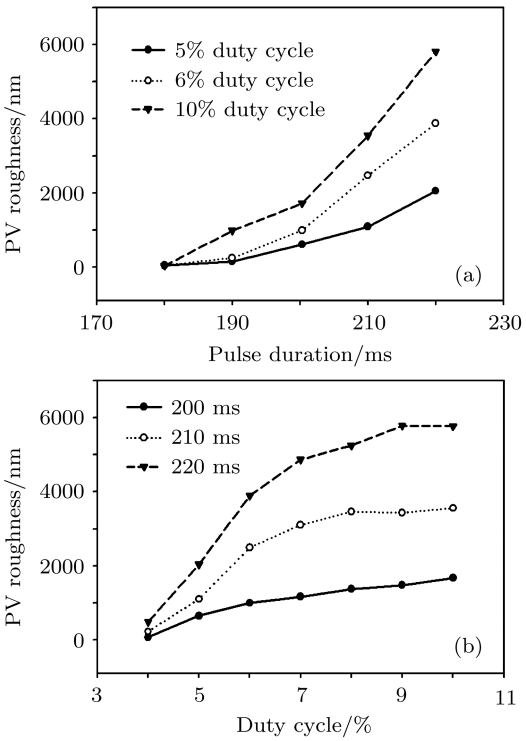


Fig. 6. Surface PV roughness of the laser irradiated area as a function of (a) pulse duration and (b) duty cycle.

4. Conclusion

Three typical surface morphologies and two typical hydrophilicity test images are observed at different surface temperatures induced by various laser powers and pulse durations on the fused silica. The different hydrophilicity behaviours are related to surface structures of the laser-induced crater and thermal diffusion area. The thermal diffusion length monotonously increases with increasing laser power and pulse duration. The crater width is almost determined by the laser beam size. The crater depth is more sensitive to the laser power and pulse duration than the crater width.

References

[1] Miller P E, Suratwala T I, Wong L L, Feit M D, Menapace J A, Davis P J and Steele R A 2005 *Proc. SPIE* **5991** 599101

[2] Papernov S and Schmid A W 2008 *Proc. SPIE* **7132** 71321J

[3] Hua J R, Zu X T, Li L, Xiang X, Chen M, Jiang X D, Yuan X D and Zheng W G 2010 *Acta Phys. Sin.* **59** 2519 (in Chinese)

[4] Wang F R, Huang J, Liu H J, Zhou X D, Jiang X D, Wu W D and Zheng W G 2010 *Acta Phys. Sin.* **59** 5122 (in Chinese)

[5] Norton M A, Hrubesh L W, Wu Z, Donohue E, Feit M D, Kozlowski M R, Milam D, Neeb K P, Molander W A, Rubenchik A M, Sell W D and Wegner P 2000 *Proc. SPIE* **4347** 468

[6] Bouchut P, Delrive L, Decruppe D and Garrec P 2004 *Proc. SPIE* **5252** 122

[7] Hrubesh L W, Norton M A, Molander W A, Donohue E E, Maricle S M, Penetrante B M, Brusasco R M, Grundler W, Butler J A, Carr J W, Hill R M, Summers L J, Feit M D, Rubenchik A, Key M H, Wegner P J, Burnham A K, Hackel L A and Kozlowski M R 2002 *Proc. SPIE* **4679** 23

[8] Bouchut P, Garrec P and Pelle C 2003 *Proc. SPIE* **4932** 103

[9] Feit M D and Rubenchik A M 2003 *Proc. SPIE* **4932** 91

[10] Feit M D, Rubenchik A M, Boley C D and Rotter M 2004 *Proc. SPIE* **5273** 145

[11] Gallais L, Cormont P and Rullier J L 2009 *Opt. Express* **17** 23489

[12] Bass I L, Guss G M and Hackel R P 2005 *Proc. SPIE* **5991** 59910C

[13] Bass I L, Draggoo V G, Guss G M, Hackel R P and Norton M A 2006 *Proc. SPIE* **6261** 62612A

[14] During A, Bouchut P, Coutard J G, Leymarie C and Bercegol H 2007 *Proc. SPIE* **6403** 640323

[15] Guss G, Bass I, Draggoo V, Hackel R, Payne S, Lancaster M and Mak P 2007 *Proc. SPIE* **6403** 64030M

[16] Philipp H R 1971 *J. Phys. Chem. Solids* **32** 1935

[17] Skuja L 1998 *J. Non-cryst. Solids* **239** 16

[18] Temple P A, Lowdermilk W H and Milam D 1982 *Appl. Opt.* **21** 3249

[19] Brusasco R M, Penetrante B M, Butler J A, Maricle S M and Peterson J E 2002 *Proc. SPIE* **4679** 34

[20] Palmier S, Gallais L, Commandré M, Cormont P, Courchinoux R, Lamaignère L, Rullier J L and Legros P 2009 *Appl. Surf. Sci.* **255** 5532

[21] Mclachlan A D and Meyer F P 1987 *Appl. Opt.* **26** 1728